Blood Cells, Molecules, and Diseases xxx (2009) xxx–xxx

Contents lists available at ScienceDirect

Blood Cells, Molecules, and Diseases

journal homepage: www.elsevier.com/locate/ybcmd

Spatial analysis of erythrocyte membrane fluctuations by digital holographic microscopy

Benjamin Rappaz [a], Alexander Barbul [b], Annick Hoffmann [a], Daniel Boss [a,d], Rafi Korenstein [b], Christian Depeursinge [c], Pierre J. Magistretti [a,d], Pierre Marquet [a,d,*]

[a] Brain Mind Institute, École Polytechnique Fédérale de Lausanne, 1015 Lausanne, Switzerland
[b] Department of Physiology and Pharmacology, Sackler Faculty of Medicine, Tel Aviv University, Tel Aviv, Israel
[c] Ecole Polytechnique Fédérale de Lausanne, Laboratoire d'Optique Appliquée, 1015 Lausanne, Switzerland
[d] Centre de Neurosciences Psychiatriques, Département de psychiatrie DP-CHUV, Site de Cery, 1008 Prilly-Lausanne, Switzerland

ARTICLE INFO

Article history:
Submitted 5 January 2009
Available online xxxx

(Communicated by
J.F. Hoffman, Ph.D., 06 January 2009)

Keywords:
Cell membrane fluctuations
Red blood cell
Digital holography
Quantitative phase microscopy
Refractive index

ABSTRACT

Red blood cell (RBC) membrane fluctuations provide important insights into cell states. We present a spatial analysis of red blood cell membrane fluctuations by using digital holographic microscopy (DHM). This interferometric and dye-free technique, possessing nanometric axial and microsecond temporal sensitivities enables to measure cell membrane fluctuations (CMF) on the whole cell surface. DHM acquisition is combined with a model which allows extracting the membrane fluctuation amplitude, while taking into account cell membrane topology. Uneven distribution of CMF amplitudes over the RBC surface is observed, showing maximal values in a ring corresponding to the highest points on the RBC torus as well as in some scattered areas in the inner region of the RBC. CMF amplitudes of 35.9 ± 8.9 nm and 4.7 ± 0.5 nm (averaged over the cell surface) were determined for normal and ethanol-fixed RBCs, respectively.

Introduction

The red blood cell membrane possesses particular mechanical characteristics which enables it to undergo large deformation when passing through narrow capillaries. Understanding the origin of cell membrane fluctuations may provide information about the functional status of erythrocyte under normal and pathological conditions.

There are two types of forces that were suggested to drive cell membrane fluctuations. The first is thermal motion [1,2]. The second one points to metabolic activity underlying ATP dependent mechanochemical dynamic assembly of the membrane skeleton [3] and the involvement of actin, as a part of a putative motor molecule, in this process [4,5]. Explanations for a possible coexistence of both causes for the CMF have been given. Thermally driven fluctuations are expected to be more prominent in membrane regions with small curvature, i.e. in the central region, while lower amplitudes of CMF are expected to occur in regions with high curvature, i.e. the erythrocyte rim, where the elastic membrane energy is comparatively high [6].

Different techniques including phase contrast microscopy [1], reflection interference contrast microscopy [7], light scattering technique based on point dark field microscopy [3] and recently bright-field microscopy [8] have been used to measure fluctuations of RBC membranes. However, these methods are not inherently quantitative in terms of absolute CMF measurements (often requiring interpolation of the membrane edge) and do not investigate the spatial distribution of membrane fluctuations. Basically, 3-D quantitative erythrocyte shape measurements have been limited to atomic force and scanning electron microscopies. Because of the limitations imposed by the sample preparation, these techniques have limited applicability to cells under physiological and dynamic conditions [9].

Recently, new emerging imaging approaches, called quantitative phase microscopy (QPM) have demonstrated their capability to provide accurate 3D imaging of transparent living cells [10–13]. A first attempt to measure CMF using QPM has been achieved by [11].

The QPM technique we have developed, called digital holographic microscopy (DHM) is an interferometric approach based on the holographic principle [14]. DHM allows to measure quantitatively phase shift corresponding to a few nanometers, with a high temporal stability and without using very demanding and costly opto-mechanical designs as required by conventional interferometric techniques. DHM allows not only visualization of transparent biological specimens but also provides quantitative information about cell morphology [12,15].

In this study, DHM was used to measure the refractive index of individual living erythrocyte and to quantify the erythrocyte membrane fluctuations amplitude over the whole cell surface in normal and ethanol-fixed cells. Practically, the calculation of the CMF was achieved

* Corresponding author.
E-mail address: p.marquet@a3.epfl.ch (P. Marquet).

1079-9796/$ – see front matter © 2009 Elsevier Inc. All rights reserved.
doi:10.1016/j.bcmd.2009.01.018

taking into account the membrane orientation, the refractive index value of the cells and by subtracting measured background noise.

Methods

Cell preparation

Cells were prepared according to [16]. In short: 100–150 µl of blood was drawn from healthy laboratory personnel by fingerpick, collected and diluted at a ratio of 1:10 (v/v) in cold HEP buffer (15 mM HEPES pH 7.4, NaCl 130 mM, KCl 5.4 mM and 10 mM glucose). Blood cells were sedimented at 200 *g*, 4 °C for 10 min and buffy coat was gently removed. Red blood cells were washed twice in HEP buffer (1000 *g* × 2 min at 4 °C). Finally, erythrocytes were suspended in HEPA buffer (15 mM HEPES pH 7.4, 130 mM NaCl, 5.4 mM KCl, 10 mM glucose, 1 mM $CaCl_2$, 0.5 mM $MgCl_2$ and 1 mg/ml bovine serum albumin) at 0.2% hematocrit. The erythrocyte suspension was introduced into a closed experimental chamber consisting of two cover glasses separated by spacers 1.2 mm thick, and incubated for 20 min at 37 °C. This allows the erythrocytes to adhere to the glass coverslip.

The chamber was then mounted on the DHM stage and holograms were acquired and numerically reconstructed on-line using a custom-made C++ software [17]. Neither erythrocyte shape transitions nor volume changes were detected during the experiment. All experiments were conducted at room temperature (~22 °C). For the decoupling procedure presented later the cells were deposed in a dedicated perfusion chamber [18] and either 60 mM mannitol or 60 mM Nycodenz (Histodenz, Sigma) was added to the HEPA buffer. In addition water was added to preserve the osmolarity of 298 mOsm (measured with a freezing-point osmometer (Roebling, Germany)). For ethanol fixation, the cells were deposed on a coverslip, fixed with 90% ethanol and rinse twice with HEPA buffer, before being mounted on the DHM stage.

Digital holographic microscope setup

The experimental setup is a modified Mach–Zehnder configuration (Fig. 1). Light transmitted by the specimen and collected by a Leica HCX PL APO 100×, NA = 1.4, oil microscope objective (MO) forms the object wave *O*, which interferes with a reference wave *R* to produce the hologram intensity I_H recorded by the digital camera (Fig. 1B). Holograms are recorded in an off-axis geometry i.e. the reference wave reaches the CMOS camera (Sniper F-50, Akateck) with a small incidence angle (~1°) with respect to the propagation direction of the object wave.

A detailed description of the algorithm used for hologram reconstruction in such an off-axis configuration and aberration compensation has been previously described in [17,19].

Briefly, the reconstruction procedure consists in a numerical calculation of the hologram re-illumination by a digital reference wave and a numerical correction of the wave front aberrations induced by the objective and by the off-axis geometry. Such a reconstruction process also allows to correct wave front aberration [20] and to compensate for experimental noise (time drift, vibration, etc.) therefore assuring a high phase stability making possible to explore biological processes occurring on the microsecond to hours time scale.

The acquisition time is currently limited by the exposure time of the camera (down to ~20 µs) and the intensity of the irradiating source. The reconstruction process is achieved in real-time (>15 images/s) using a standard PC computer (Pentium IV, 3.2 GHz). For experiments requiring higher hologram acquisition rates, the reconstruction is achieved off-line at the end of the experiment.

256*256 pixels were acquired at the maximal camera speed (~102 Hz). To reduce noise a temporal summation of 4 images was applied (leading to a final acquisition frequency of ~25 Hz) and a spatial summation of 2*2 pixels was also achieved (giving a 106 nm lateral resolution, higher than the diffraction spot of the MO used).

Decoupling procedure

The procedure used to separately measure the cell refractive index and thickness was described in detail in [16]. In brief, it consists of measuring cell phase mapping, sequentially, in two iso-osmolar perfusion solutions of different refractive indices. Specifically, the refractive index of the second solution is increased by replacing mannitol by Nycodenz. The procedure of exchange of the extracellular medium was repeated three times to improve measurement accuracy.

An extensive quality assurance of the DHM technique has been published in [16].

Results

Refractive index measurement

We measured the refractive index (RI) of 13 erythrocytes and found a very stable value amongst different cells of $n = 1.394 \pm 0.008$ (STD). This measured mean refractive index lies within the reported range of 1.37 to 1.42 [16] and our previous measurements [16]. Repetitive measurement of the same cell showed a constant RI over the recording period (lower than measurement accuracy).

Membrane fluctuations

Amplitude analysis

To assess the amplitude of membrane fluctuations the phase temporal fluctuations – defined as the standard deviation of the phase signal of a point in the image during a defined recording time period –

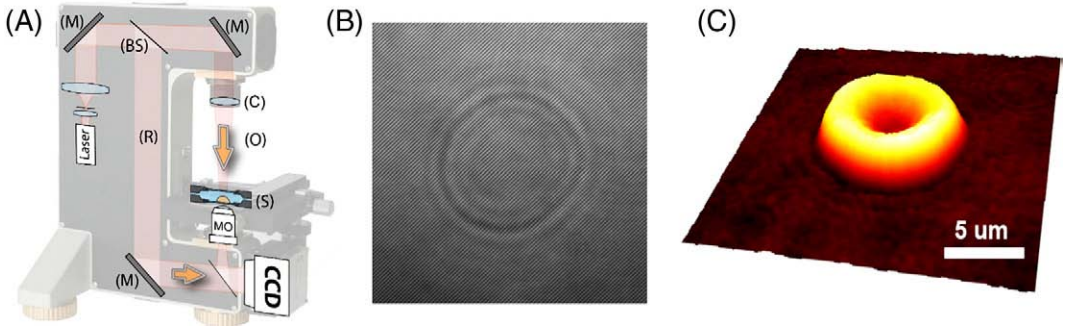

Fig. 1. (A) Basic configuration for digital holographic microscopy (DHM). A laser diode produces the coherent light (λ = 683 nm) which is divided by a beam splitter (BS). The specimen (S) is illuminated by one beam through a condenser. The microscope objective (MO) collects the transmitted light and forms the object wave (O) which interferes with a reference beam (R) to produce the hologram recorded by the CMOS camera. The sample is mounted in a chamber used for recording. (B) Typical example of a hologram acquired by the camera (256 × 256 pixels). (C) 3D representation of a quantitative phase image of an erythrocyte. Color scale in degree. (For interpretation of the references to colour in this figure legend, the reader is referred to the web version of this article.)

Please cite this article as: B. Rappaz, et al., Spatial analysis of erythrocyte membrane fluctuations by digital holographic microscopy, Blood Cells Mol. Dis. (2009), doi:10.1016/j.bcmd.2009.01.018

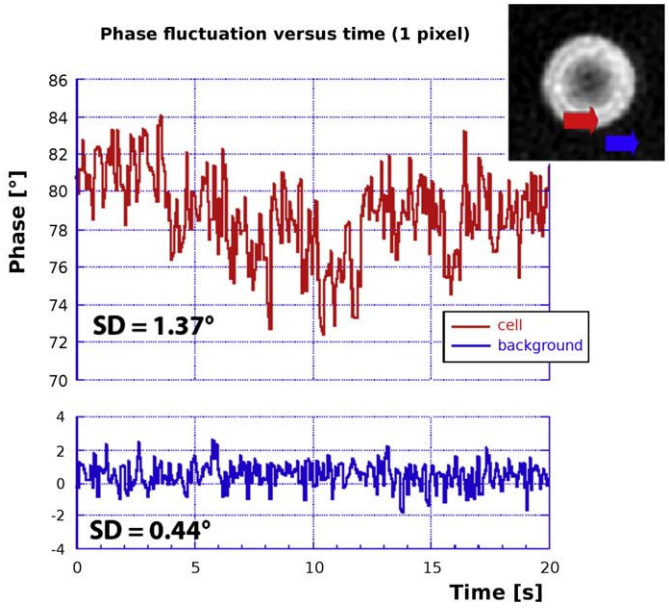

Fig. 2. Phase signals of two different regions (1 pixel region outside the cell (blue) and within the cell (red)) recorded at 25 Hz during a 10 s period. The standard deviations of the signal are 0.44° and 1.37°, respectively. Inset: phase image of the monitored erythrocyte with the corresponding regions indicated by color arrows. (For interpretation of the references to colour in this figure legend, the reader is referred to the web version of this article.)

of a region within the erythrocyte has been compared with a region outside the erythrocyte, serving as a control signal. A control experiment with a laser scanning confocal microscope (LSCM) showed that the lower membrane of the cell is attached to the glass coverslip and thus does not contribute to membrane fluctuations (data not shown).

Phase signals were recorded during 20s. Membrane fluctuation is measured in terms of temporal phase variation. The measured standard deviations of the pixel inside and outside the cell are 0.44° and 1.37°, respectively, indicating membrane fluctuation amplitudes significantly larger than the background noise level (Fig. 2).

The fluctuation phase signal recorded within the cell perimeter depends on both the parasitic phase fluctuations (associated to liquid movement or vibration, noise from the CMOS camera, air turbulence, etc.) estimated by the phase signal measured outside the cell perimeter, and on the actual membrane fluctuations. Consequently, the temporal variance of the phase signal recorded in the cell, $Var(\varphi_{cell}+\varphi_{background})$, can be expressed by:

$$Var\left(\varphi_{cell}+\varphi_{background}\right) = Var(\varphi_{cell}) + Var\left(\varphi_{background}\right) + 2Cov\left(\varphi_{cell},\varphi_{background}\right), \quad (1)$$

where $Var(\varphi_{cell})$, $Var(\varphi_{backgroundl})$ are the temporal variance corresponding to the cell membrane fluctuations and to the parasitic phase fluctuation respectively and $Cov(\varphi_{cell},\varphi_{backgroundl})$ is the covariance of the two variables. Assuming that the two variables are independent, $Cov(\varphi_{cell},\varphi_{backgroundl})=0$, which is a proper hypothesis for a weakly diffracting object such as a living cell. Thus, according to Eq. (1), the temporal deviation of each pixel $std(\varphi_{cell})_{(x,y)}$ can be evaluated by:

$$std(\varphi_{cell})_{(x,y)} = \sqrt{\left(std\left(\varphi_{cell}+\varphi_{background}\right)_{(x,y)}\right)^2 - \left(std\left(\varphi_{background}\right)\right)^2}, \quad (2)$$

where $std(\varphi_{cell}+\varphi_{background})_{(x,y)}$ is the measured temporal deviation within the cell (combining both the cell fluctuations and noise) and $std(\varphi_{background})$ is the mean of the temporal deviation of all the pixels outside the cell perimeter. The membrane fluctuations amplitude is then derived from the deviation map (in degree), with the following equation:

$$CMF(nm)_{(x,y)} = \frac{std(\varphi_{cell})[^\circ]_{(x,y)} \times \lambda}{2\pi(n_{rbc}-n_{medium})}, \quad (3)$$

where $std(\varphi_{cell})[^\circ]_{(x,y)}$ is the deviation map expressed in degree, λ is the light source wavelength, n_{rbc} and n_{medium} are the refractive indices of the RBC and medium, respectively. A representative raw CMF fluctuation map, in nanometer, is shown in Fig. 3 (B).

In the raw image (Fig. 3B) we observe large fluctuations at the cell border and around the center of the cell. In these regions the membrane has a high slope, thus a small lateral displacement of the cell membrane have a strong impact on the phase value as phase signal measures variations along the z-axis (blue vector in Fig. 3C). In order to avoid systematic overvaluing the cell fluctuations in the high-slope areas, it is necessary to evaluate the cell fluctuations in a direction perpendicular (normal) to the cell membrane (green vector in Fig. 3C). Practically, normal fluctuations have been estimated by multiplying the raw image by the cosine of the angle α (Fig. 4, top-right), evaluated from the cell thickness image in Fig. 3A.

Local movements normal to the cell membrane plane are also measured in approaches based on interpolation of the cell edge [8,21]. Our analysis complements the analysis of previous studies by providing information on the movement of the cell in regions other than the cell edge.

The blue ring around the cell (bottom-right image in Fig. 4) corresponds to regions where the cell signal passes through the area of the cell edge, which is not in contact with the coverslip (observed by LSCM) and is thus not correctly modeled by our approach. Such regions were not taken into account in further analysis.

The other regions within the RBC show a rather constant normal fluctuation amplitude (after membrane orientation correction) of about 35.9 ± 8.9 nm (mean $\pm$ SD, $n=9$ cells), within the range of previously measured values of 52.6 nm [21], 46.8 nm [22] and 23.6 nm [8]. As a control we employed 90% ethanol-fixed cells. As expected we obtained negligible CMF of 4.7 ± 0.5 ($n=6$) close to the sensitivity of

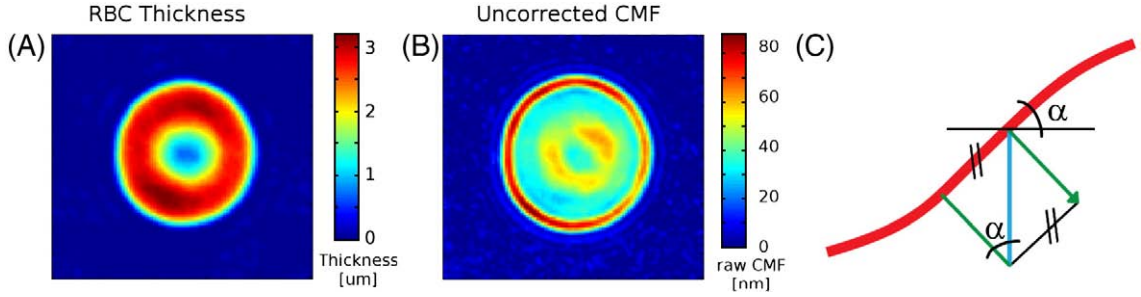

Fig. 3. (A) Thickness representation of a representative RBC, z-axis in μm, (B) Raw membrane fluctuations amplitude for the same RBC, z-axis denotes membrane fluctuations amplitude in nm, (C) Model of the different parts of the fluctuation. Angle α is defined as the angle between the membrane and the horizontal plane.

Please cite this article as: B. Rappaz, et al., Spatial analysis of erythrocyte membrane fluctuations by digital holographic microscopy, Blood Cells Mol. Dis. (2009), doi:10.1016/j.bcmd.2009.01.018

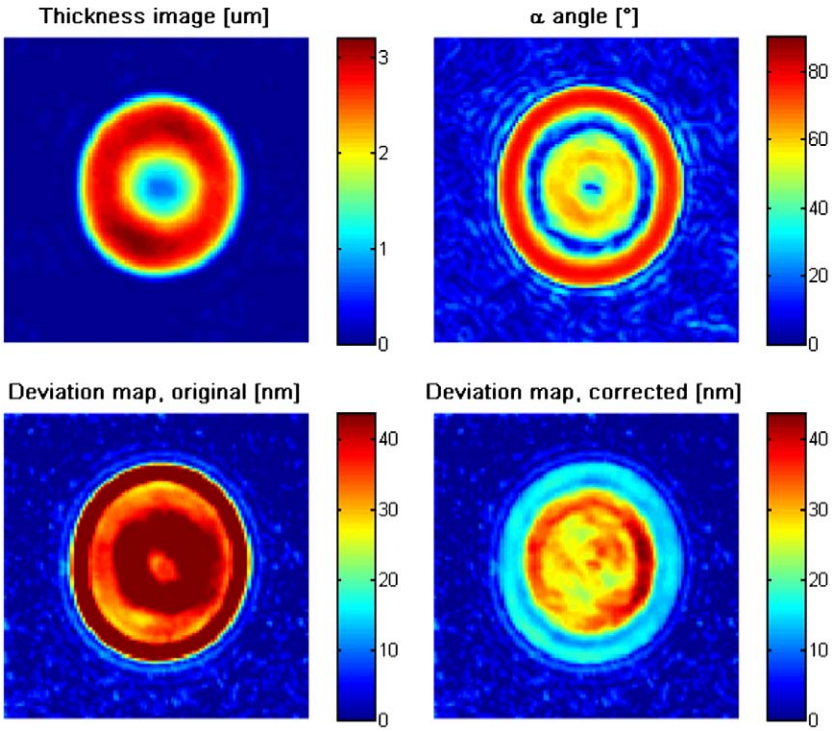

Fig. 4. Summary of the fluctuations amplitude analysis on a representative normal cell. Top left: cell thickness obtained with the decoupling procedure. Top right: maximum angle map of the RBC membrane (α in Fig. 3C). Bottom left: raw membrane fluctuation amplitude and bottom right: corrected membrane fluctuations amplitude (the two bottom images have the same colorscale). (For interpretation of the references to colour in this figure legend, the reader is referred to the web version of this article.)

the DHM (Fig. 5). It should however be stressed that the measured cell membrane fluctuations with amplitude of 36 nm (average over the whole surface), were obtained under conditions confined to the frequency range of 0.2–12 Hz.

Assuming that the membrane–cytoskeleton structural elements of the erythrocyte are evenly distributed, a homogenous spreading of fluctuation amplitudes over the cell surface would be anticipated. However, one clearly observes uneven distribution of amplitudes having maximal values in a ring corresponding to the highest points on the RBC torus, as well as in some scattered areas in the inner region of the RBC. Moreover, attributing Brownian motion as the sole driving force for CMF one would expect to have higher fluctuation amplitudes in the planar mechanically unstrained membrane at the cell center, as compared to the mechanically strained curved region on the RBC torus. The fact that the opposite is observed may point out to the possible involvement of unevenly distributed putative molecular motors.

Discussion

Digital holographic microscopy is a full field optical interferometric technique not requiring scanning and allowing to visualize, without labeling procedure, transparent objects including living cells with a nanometric axial sensitivity over the milliseconds time domain. Basically, very small phase shifts produced by living cells provide information about cell morphology as well as on the intracellular refractive index related to the cell content. Thanks to decoupling procedure and the fast acquisition time, the DHM phase signal allows to calculate important red blood cell parameters including mean corpuscular volume, mean corpuscular hemoglobin concentration as well as to efficiently address the important issue of the erythrocyte flickering.

This method provides new insights into the dynamics of the red blood cells and will be further used to investigate the effect of physiological and pharmacological effectors on RBCs.

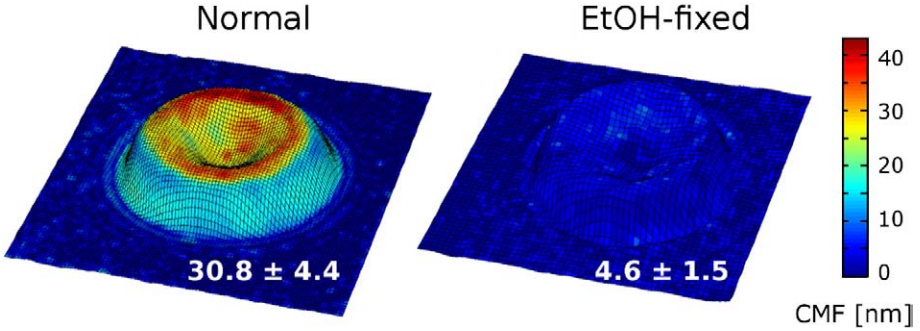

Fig. 5. Normal cell membrane fluctuations displayed as color-code over the shape of the RBC for a representative normal and ethanol-fixed cells. Insets contain the mean ± SD [nm] of the CMF of the analyzed regions for each representative cell. (For interpretation of the references to colour in this figure legend, the reader is referred to the web version of this article.)

Please cite this article as: B. Rappaz, et al., Spatial analysis of erythrocyte membrane fluctuations by digital holographic microscopy, Blood Cells Mol. Dis. (2009), doi:10.1016/j.bcmd.2009.01.018

Acknowledgments

The authors would like to thanks Corinne Moratal for her technical assistance and the personnel of Lyncée Tec SA (www.lynceetec.com), PSE-A, CH-1015 Lausanne, Switzerland, for their technical support and the fruitful discussions during the course of the experimentation. This work has been supported by the Swiss National Science Foundation (grant 205320-112195/1) and CTI project 9389.1. A.B. has been supported by Nano2life European Network of Excellence travel grants. Aspects of this article were presented in the 2008 Red Cell Conference held at the University of Rochester, New York, in memory of Philip Knauf.

References

[1] F. Brochard, J.F. Lennon, Frequency spectrum of flicker phenomenon in erythrocytes, J. Phys. 36 (1975) 1035–1047.
[2] H. Strey, M. Peterson, Measurement of erythrocyte-membrane elasticity by flicker eigenmode decomposition, Biophys. J. 69 (1995) 478–488.
[3] S. Levin, R. Korenstein, Membrane fluctuations in erythrocytes are linked to MgATP-dependent dynamic assembly of the membrane skeleton, Biophys. J. 60 (1991) 733–737.
[4] S. Tuvia, A. Almagor, A. Bitler, et al., Cell membrane fluctuations are regulated by medium macroviscosity: evidence for a metabolic driving force, Proc. Natl. Acad. Sci. U. S. A. 94 (1997) 5045–5049.
[5] S. Tuvia, S. Levin, A. Bitler, R. Korenstein, Mechanical fluctuations of the membrane-skeleton are dependent on F-actin ATPase in human erythrocytes, J. Cell Biol. 141 (1998) 1551–1561.
[6] R. Korenstein, S. Tuvia, L. Mittelman, S. Levin, Local bending fluctuations of the cell membrane, in: N. Akkas (Ed.), Biomechanics of Active Movement and Division of Cells, 33, Springer-Verlag Berlin, Berlin, 1994, pp. 415–423.
[7] A. Zilker, H. Engelhardt, E. Sackmann, Dynamic reflection interference contrast (Ric—) microscopy — a new method to study surface excitations of cells and to measure membrane bending elastic-moduli, J. Phys. 48 (1987) 2139–2151.
[8] J. Evans, W. Gratzer, N. Mohandas, et al., Fluctuations of the red blood cell membrane: relation to mechanical properties and lack of ATP dependence, Biophys. J. 94 (2008) 4134–4144.
[9] R. Nowakowski, P. Luckham, P. Winlove, Imaging erythrocytes under physiological conditions by atomic force microscopy, Biochim. Biophys. Acta-Biomembr. 1514 (2001) 170–176.
[10] D. Carl, B. Kemper, G. Wernicke, G. von Bally, Parameter-optimized digital holographic microscope for high-resolution living-cell analysis, Appl. Opt. 43 (2004) 6536–6544.
[11] G. Popescu, T. Ikeda, C.A. Best, et al., Erythrocyte structure and dynamics quantified by Hilbert phase microscopy, J. Biomed. Opt. 10 (2005) 060503.
[12] P. Marquet, B. Rappaz, P.J. Magistretti, et al., Digital holographic microscopy: a noninvasive contrast imaging technique allowing quantitative visualization of living cells with subwavelength axial accuracy, Opt. Lett. 30 (2005) 468–470.
[13] C. Curl, C. Bellair, P. Harris, et al., Single cell volume measurement by Quantitative Phase Microscopy (QPM): a case study of erythrocyte morphology, Cell. Physiol. Biochem. 17 (2006) 193–200.
[14] D. Gabor, A new microscopic principle, Nature 161 (1948) 777–778.
[15] B. Rappaz, F. Charriere, C. Depeursinge, et al., Simultaneous cell morphometry and refractive index measurement with dual-wavelength digital holographic microscopy and dye-enhanced dispersion of perfusion medium, Opt. Lett. 33 (2008) 744–746.
[16] B. Rappaz, A. Barbul, Y. Emery, et al., Comparative study of human erythrocytes by digital holographic microscopy, confocal microscopy, and impedance volume analyzer, Cytometry A 73 (2008) 895–903.
[17] T. Colomb, F. Montfort, J. Kuhn, et al., Numerical parametric lens for shifting, magnification, and complete aberration compensation in digital holographic microscopy, J. Opt. Soc. Am. A-Opt. Image Sci. Vis. 23 (2006) 3177–3190.
[18] B. Rappaz, P. Marquet, E. Cuche, et al., Measurement of the integral refractive index and dynamic cell morphometry of living cells with digital holographic microscopy, Opt. Express 13 (2005) 9361–9373.
[19] E. Cuche, P. Marquet, C. Depeursinge, Simultaneous amplitude-contrast and quantitative phase-contrast microscopy by numerical reconstruction of Fresnel off-axis holograms, Appl. Opt. 38 (1999) 6994–7001.
[20] T. Colomb, J.K. Kuhn, F. Charriere, et al., Total aberrations compensation in digital holographic microscopy with a reference conjugated hologram, Opt. Express 14 (2006) 4300–4306.
[21] A. Bitler, A. Barbul, R. Korenstein, Detection of movement at the erythrocyte's edge by scanning phase contrast microscopy, J. Microsc. (Oxford) 193 (1999) 171–178.
[22] G. Popescu, T. Ikeda, R.R. Dasari, M.S. Feld, Diffraction phase microscopy for quantifying cell structure and dynamics, Opt. Lett. 31 (2006) 775–777.

Please cite this article as: B. Rappaz, et al., Spatial analysis of erythrocyte membrane fluctuations by digital holographic microscopy, Blood Cells Mol. Dis. (2009), doi:10.1016/j.bcmd.2009.01.018